

Numerical Study of Mixed Convection in Baffled Vented Cavity

Yawovi Nougbléga^{1,*}, Koffi Sagna², Kossi Atchonouglo¹

¹Laboratoire Sur l'Energie Solaire /Groupe Phénomène de Transfert et Energétique - Université de Lomé

²Laboratoire Sur l'Energie Solaire /Chair Unesco sur les Energies Renouvelables - Université de Lomé

*Corresponding author: nycogl@yahoo.fr

Received November 18, 2019; Revised December 21, 2019; Accepted December 30, 2019

Abstract Mixed convection is numerically studied in a baffled vented cavity with constant heat flux from a uniformly heated left vertical wall. An external airflow enters the cavity through the inlet opening in the right vertical wall and exits from the outlet opening in the opposite wall. The two-dimensional mathematical model includes a system of five governing partial differential equations of continuity, linear momentum and energy, discretized by the finite difference method, and solved by the Thomas algorithm and the Gauss Seidel Method. Flow and thermal fields are investigated by numerical simulations of air cooling with a Reynolds number in the range $10 \leq Re \leq 200$, and Rayleigh number: $10^4 \leq Ra \leq 10^6$. Three different locations of the two heated baffles are used in the configurations to analyze the effect of heat transfer in terms of streamlines, local Nusselt number, velocity and isotherms within the three configurations. The results show that the locations of the heated baffles along the horizontal walls enable to create simultaneously the isolated zone and the heated zone in the baffled vented cavity.

Keywords: heated baffle, vented cavity, isolated zone, passive cooling, heat enhancement

Cite This Article: Yawovi Nougbléga, Koffi Sagna, and Kossi Atchonouglo, "Numerical Study of Mixed Convection in Baffled Vented Cavity." *International Journal of Physics*, vol. 8, no. 1 (2020): 1-10. doi: 10.12691/ijp-8-1-1.

1. Introduction

Mixed convection heat transfer in ventilated systems continues to be a fertile area of research, due to the interest of the phenomenon in many technological processes, such as the design of solar collectors, thermal design of buildings, air conditioning and recently the cooling of electronic circuit boards. The need for effective cooling in the electronic industry has put a limit on the application of conventional cooling methods like natural convection. This is one of the main reasons that mixed convection or combined forced and free convection has gained popularity over the years and will continue to do so with the size of all electronic devices shrinking drastically every day. Not only in the electronic industry but the nuclear, solar, bio-medical are some of the diverse fields that employ mixed convection. Thus, its study is of paramount importance and today the focus is more on different techniques for enhancing heat transfer in mixed convective flow rather than an employing simple mixed convective flow. In electronic devices, there exist channels that often have protruding or flush mounted heaters. Du et al (1998) [1] reviewed the literature on the study of flush mounted heaters in channels undergoing mixed convection. The geometrical form used in (How & Hsu 1998) [2] was that of a square enclosure having a constant-flux heat source in the left vertical wall with the upper opening on the same side and an exit on the

opposite side. A conducting baffle acting as a divider was placed either on the top wall or in the bottom wall. Hsu & How (1999) [3] investigated the problem of mixed convection in which the geometry and wall temperature conditions were similar to that of (How & Hsu 1998) [2] but it had a square heat conducting body located within the enclosure, unlike a baffle on the wall as in (How & Hsu 1998) [2]. El-din (2002) [4] investigated mixed convection in a vertical channel divided into two passages by means of a conductive baffle. Previous studies on mixed convection for U-shaped open cavities have been extensively reviewed by Manca et al (2003, 2008) [5]. A numerical investigation was carried out by Singh & Sharif (2003) [6], in which a rectangular cavity with differentially heated side walls for different positions of inlet and outlet openings for the forced air and also different wall temperature conditions hot or cold was considered. A cavity having finite length slots midway on the two vertical walls (left and right) and a constant heat flux source located on the left vertical wall with all other walls perfectly insulated was considered by Raji et al (2008) [7]. A ventilated rectangular partitioned cavity was the geometry considered by Bahlaoui et al (2009) [8] in which the combined effect of mixed convection and radiation was investigated. The application of baffles in the channel or cavity has once again received considerable attention over the past few years. Chang & Shiau (2005) [9] investigated the effect of pulsating flow in a vertical open channel having a horizontal thin baffle at the right wall and a finite length of left wall heated by a constant heat

flux. Three Baffles for aiding the mixing process in a micro-mixer was implemented in Chung et al (2008) [10]. The dependence of mixing efficiency on baffle height and Reynolds number was investigated in this study. Numerical studies on a ventilated cavity having a central heater near the inlet, on the lower left wall and having an exit at the upper right wall was studied by Radhakrishnan et al (2009) [11]. Here, the effect of a baffle an increasing heat transfer was investigated, also the best position of the baffle among bottom, left, right and top was found in which heat transfer rate was enhanced by 50% as compared to the case of a no-baffle. Asif et al (2011) [12] also numerically studied a ventilated cavity but here three isothermally heated baffles were placed alternately in the left and right walls. A Horizontal Channel with two diamond-shaped baffles placed on the lower and upper walls in a staggered array was the geometrical form considered by Sripattanapipat & Promvonge (2009) [13]. A numerical and experimental study on z-shaped baffles in a turbulent regime was conducted by Sriromreun et al (2012) [14]. The above review of the literature highlights the importance studies on mixed convection in a cavity or a channel as shown by Singh & Sharif (2003) [6] and Manca et al (2003, 2008) [5, 15]. The concept of using a baffle or a divider is very old and previous studies like How & Hsu (1998) [2] investigated the effect of a change in baffle height and location on heat transfer in such geometries. However, over the years, there has been a

renewed interest in the use of baffles in geometries. Recent studies in mixed convection in cavities or channels with baffles have different applications like in Chung et al (2008) [10], where mixing was the prime objective. Still, most of the studies had the prime objective of increasing heat transfer when employing baffles. Studies by Radhakrishnan et al (2009) [11], Asif et al (2011) [12] dealt with the effect of a baffle in a ventilated cavity whereas Sripattanapipat & Promvonge (2009) [13]; Sriromreun et al (2012) [14] dealt with the effect of different shapes of the baffles in simple channels.

The literature review shows clearly that, no work has been done on the emplacement of a thermally heated baffle in the vented cavity for enhancing heat transfer for effective cooling in the electronic box. Due to the practical interest of this problem in a wide variety of engineering applications of passive cooling, the subject needs further attention to improve knowledge in this field.

The present numerical study is an effort to analyze firstly flow and heat transfer in a differentially heated vented cavity, where two thermally heated baffles are placed at the top and the bottom horizontal walls. The reason for placing the baffles is to enhance heat transfer by diverting forced flow from the inlet opening to the exit at the top of the right heated wall. In the present study, a range of Rayleigh numbers $Ra = 10^4$ to 10^6 and different Re (10 to 200), are considered. Also the location and height of the thermally heated baffles on the top and bottom horizontal walls are varied.

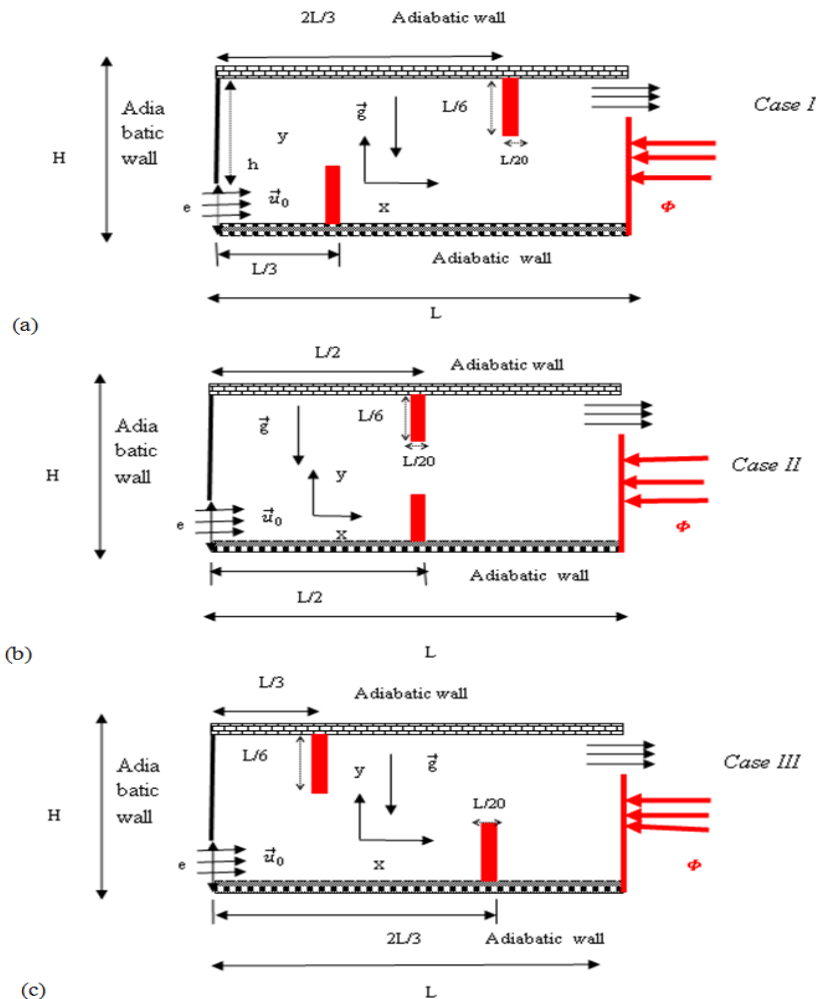


Figure 1. Physical model [(a) Baffles left- right ($L/3$; $2L/3$) (b) Baffles center – center ($L/2$; $L/2$) (c) Baffles right- left ($L/3$; $2L/3$)]

2. Problem Formulation

The three different configurations of the two-dimensional cavity model under study with the system of coordinates are sketched in Figure 1. It consists of the vented cavity heated by a uniform heat flux from its vertical right wall while the remaining walls are considered perfectly adiabatic. The rectangular cavity has a geometrical aspect ratio $AR=2$. The cavity is divided by two heated baffles located at three different positions along the horizontal walls. The baffles have width $e_b=L/20$, height $H_b=L/6$. The system is subjected to an imposed flow of fresh air, parallel to the horizontal walls, entering the cavity from the inlet opening located at the bottom of the left vertical wall of the cavity and leaving through the outlet opening.

The numerical simulations are based on the assumption that the temperature difference between the heated baffles and the left vertical active wall is not very high so that the Boussinesq approximation is valid. The flow is considered to be incompressible, laminar and two-dimensional. The transport properties of the fluid are kept constant and the effect of viscous dissipation is neglected. Considering the above-mentioned assumptions, the dimensionless form of governing equations, written in vorticity – streamlines ($\omega-\psi$) formulation, are as follows:

$$\frac{\partial U}{\partial X} + \frac{\partial V}{\partial Y} = 0 \quad (1)$$

$$\left\{ \begin{array}{l} X = 0 \text{ and } 0 < Y < E; U = 1, \psi = Y, V = \omega = \theta = 0 \\ X = 0 \text{ and } E < Y < 1; U = V = \psi = 0, \omega = -\frac{\partial^2 \psi}{\partial x^2} \Big|_{X=0}, \frac{\partial \theta}{\partial X} \Big|_{X=0} = 0 \\ X = A \text{ and } 0 < Y < D; U = V = \psi = 0, \omega = -\frac{\partial^2 \psi}{\partial X^2} \Big|_{X=A}, \frac{\partial \theta}{\partial x} \Big|_{X=A} = 1 \\ X = A \text{ and } D < Y < 1; \frac{\partial \theta}{\partial Y} \Big|_{X=A} = \frac{\partial \psi}{\partial Y} \Big|_{X=A} = \frac{\partial \omega}{\partial Y} \Big|_{X=A} = \frac{\partial U}{\partial Y} \Big|_{X=A} = \frac{\partial V}{\partial Y} \Big|_{X=A} = 0 \\ Y = 0 \text{ and } 0 < X < A; U = V = \psi = 0, \omega = -\frac{\partial^2 \psi}{\partial Y^2} \Big|_{Y=0}, \frac{\partial \theta}{\partial Y} \Big|_{Y=0} = 0 \\ Y = 1 \text{ and } 0 < X < A; U = V = \psi = 0, \omega = -\frac{\partial^2 \psi}{\partial Y^2} \Big|_{Y=1}, \frac{\partial \theta}{\partial Y} \Big|_{Y=1} = 0 \end{array} \right. \quad (7)$$

at the fluid- baffles interface the boundary conditions are written as equations (8) and (9)

$$-\lambda \frac{\partial \theta}{\partial n} = -\lambda_b \frac{\partial \theta_b}{\partial n} \quad (8)$$

$$\omega_b = -\frac{\partial^2 \psi}{\partial n^2}. \quad (9)$$

The stream function and the vorticity are related to the velocity components by the following expressions (10) to (12):

$$U = \frac{\partial \psi}{\partial Y}. \quad (10)$$

$$V = -\frac{\partial \psi}{\partial X} \quad (11)$$

$$\frac{\partial \omega}{\partial \tau} + U \frac{\partial \omega}{\partial X} + V \frac{\partial \omega}{\partial Y} = Ri \frac{\partial \theta}{\partial X} + \frac{1}{Re} \left(\frac{\partial^2 \omega}{\partial X^2} + \frac{\partial^2 \omega}{\partial Y^2} \right) \quad (2)$$

$$\frac{\partial \theta}{\partial \tau} + U \frac{\partial \theta}{\partial X} + V \frac{\partial \theta}{\partial Y} = \frac{1}{RePr} \left(\frac{\partial^2 \theta}{\partial X^2} + \frac{\partial^2 \theta}{\partial Y^2} \right) \quad (3)$$

$$\omega = -\left(\frac{\partial^2 \Psi}{\partial X^2} + \frac{\partial^2 \Psi}{\partial Y^2} \right). \quad (4)$$

The conductive heat transfer in the baffles

$$\frac{\partial \theta_b}{\partial \tau} = \frac{a_r}{RePr} \left(\frac{\partial^2 \theta_b}{\partial X^2} + \frac{\partial^2 \theta_b}{\partial Y^2} \right). \quad (15)$$

• Boundary conditions

• Initial conditions given by relation (6):

• at $\tau = 0$:

$$\theta = \omega = U = V = \psi = 0 \quad (6)$$

• at $\tau > 0$

The boundary conditions associated with the problem are found below.

At the left, right, top and bottom walls: No slip and impermeability boundary conditions have been used on the all walls except at inlet and outlet openings given by relations (7).

and

$$\omega = \left(\frac{\partial V}{\partial X} - \frac{\partial U}{\partial Y} \right) \quad (12)$$

Where the scales are defined by the relations (13):

$$\left\{ \begin{array}{l} (X, Y) = \left(\frac{x}{H}, \frac{y}{H} \right); \tau = \frac{u_{0r}}{H}; (U, V) = \left(\frac{u}{u_0}, \frac{v}{u_0} \right) \\ \Psi = \frac{\psi}{u_0 H}; \omega = \frac{\Omega H}{u_0}; \theta = \frac{\lambda(T - T_a)}{\varnothing H} \\ \theta_b = \frac{\lambda_b(T_b - T_a)}{\varnothing H}; Re = \frac{\rho u_0 (2e)}{\mu}; Gr = \frac{\rho^2 g \beta \varnothing (H)^4}{\lambda \mu^2} \end{array} \right. \quad (13)$$

and the aspect ratio expressed as: $A = L/H$; $E = e/H$; $B = h/H$, $D = (h + e)/H$.

• Evaluation of heat transfer

To evaluate the mixed convective heat transfer characteristic, the local Nusselt number is presented as:

$$Nu_w = \frac{\varnothing H}{\lambda(T_w - T_a)} = \frac{1}{\theta_w}. \quad (14)$$

The average Nusselt number is obtained using the following expression

$$Nu_m = \frac{1}{B} \int_0^B \frac{1}{\theta_w(Y)} dY. \quad (15)$$

3. Numerical Procedure of Solution

The non linear partial differential governing equations, (1-3), were discretized using a finite difference technique. The first and second derivatives of the diffusive terms were approached by central differences while a second order upwind scheme was used for the convective terms to avoid possible instabilities frequently encountered in mixed convection problems. The numerical solution of the governing equations (2-3) was assured by the Thomas algorithm. At each time step, the Poisson equation, Eq. (4), was treated using the Point Successive Under-Relaxation method (PSUR) with an optimum under-relaxation coefficient equal to 0.8 for the non uniform grid (121×81) adopted in the present study. Convergence of iteration for stream function solution is obtained at each time step. The following criterion is employed to check for steady-state solution. Convergence of solutions is assumed when the relative error for each variable between consecutive iterations is below the convergence criterion ε such that $\sum |(\phi^{k+1} - \phi^k)/\phi^{k+1}| < 10^{-5}$ where ϕ stands for ψ , θ , ω ,

k refers to time. For grid independent study, five different grid size (61×31, 81×41, 101×51, 121×61, 121×81) solutions are obtained by comparing the average Nusselt number, and the dimensionless temperature along the heated wall obtained for each grid mesh for the highest Grashof and fixed Reynolds numbers used in this work ($Gr = 10^6$ and $Re = 30$). The vorticity computational formula of (Woods, 1954) [16] for approximating wall vorticity was used: $\omega_P = \frac{1}{2}\omega_{P+1} - \frac{3}{\Delta\eta^2}(\psi_{P+1} - \psi_P)$, where ψ_P and ψ_{P+1} are stream function values at the points adjacent to the boundary wall; n is the normal abscise on the boundary wall. For the present work, the time step used in the computations is 10^{-5} and the grid size selected is (51×101).

Table 1. Grid independency

Meshes	Θ	Change(%)	Nu_m	Change(%)
61X31	0,10048	-	10,05019	-
81X41	0,10779	6.7817	9,3479	7.5128
101X51	0,1082	0.3789	9,29765	0.55404
121X61	0,11019	1.8059	9,12959	1.84083
121X81	0,11015	0.03631	9,08064	0.53906

3.1. Validation

The numerical simulations code was validated against the results of (Sumon Saha et al., 2006) [17] obtained in the case of a square cavity in which the bottom wall is subjected to a constant flux and the remaining walls are kept adiabatic. Comparisons, made in terms of streamlines and isotherms for the fixed Reynolds and thermal Richardson numbers ($Re=50$, $Ri = 1$) showed fairly good agreement.

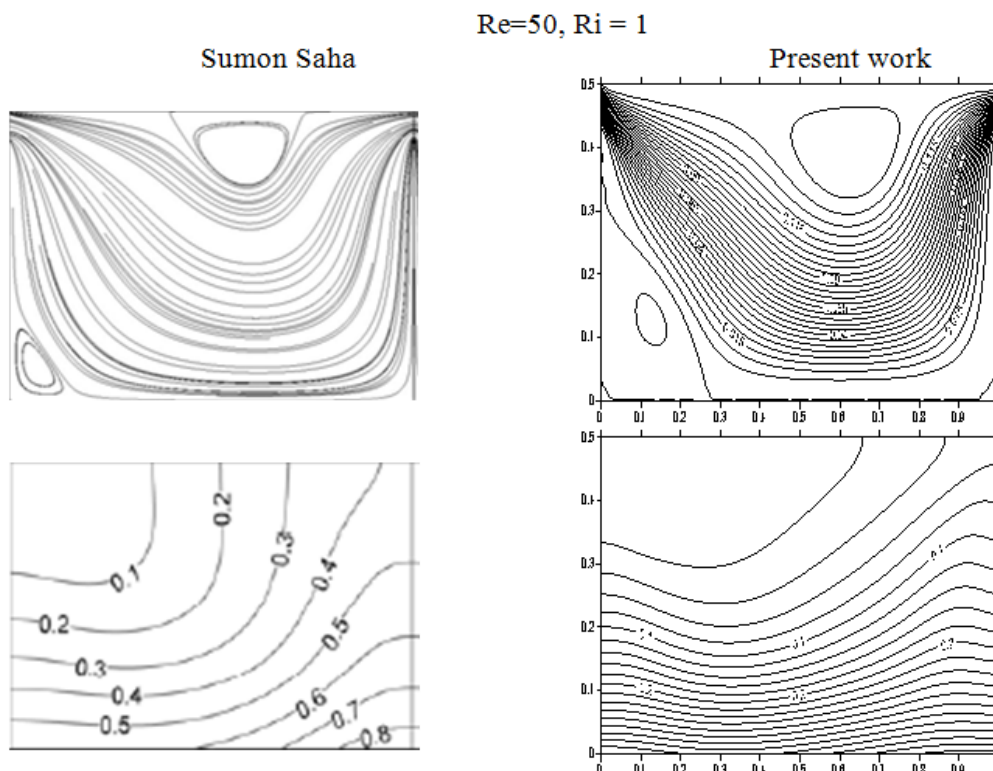


Figure 2. Comparison of streamlines and isotherms

4. Results and Discussion

The governing control parameters in the problem considered were Rayleigh (Ra), Reynolds (Re) numbers and the relative positions of the heated baffles. All these values were varied over wide ranges to study their effects on thermal transport and fluid flow phenomena. In the following, the effect of Reynolds number in the three configurations is illustrated.

4.1. Streamline and Isotherm Distribution in the Configuration Case I: Baffles Left-right ($L/3$; $2L/3$)

In the Figure 3 (a-c) the open lines appear progressively when the Reynolds number is increasing for a fixed Rayleigh number ($Ra=10^6$). The big closed cell obtained for $Re=10$ in Figure 3 (a) occupies the two zones divided by the baffles. In this situation one can conclude that the natural convection phenomenon is dominant for the high value of Reynolds number, the intensity of the formation of the enclosed cell connected to the two zones diminishes until the apparition of two closed cells separated by the upper heated baffle. This tendency indicates that there are natural recirculation cells near the heated walls in the vented cavity. The baffles play the role of enhancing the natural convective phenomenon in the vented cavity for electronic circuit boards. The shape of the isotherms indicates that the cold zone increases with Reynolds number while the isotherms are tightened near the vicinity of the right heated wall and the upper heated baffle.

4.2. Streamline and Isotherm Distribution in the Configuration Case II: Baffles Center – center ($L/2$; $L/2$)

Fig.4 (a-c) shows contours of streamlines and isotherms for different values of Reynolds number for a fixed

Rayleigh number ($Ra=10^6$) for fluid flow at the location of the heated baffles at the center of the horizontal walls. Hence in Figure 4 (a), for the low value of Reynolds number, ($Re=10$) a big closed cell seen to almost occupy whole cavity. For increasing Re , the inflow is able to break the big recirculation cell, due to the formation of two recirculation cells which are separated by the upper heated baffle. The open lines for the forced flow are still formed near the top of the lower heated baffle. The simultaneous existence of the closed cell and the open lines indicate is a manifestation of mixed convection, Figure 4 (b, c). The size of the first closed cell in front of the upper heated baffle is smaller than the size of the second closed cell located between the upper heated baffle and the left vertical heated wall. The position of the two closed cells indicated that the central position of the heated baffles in the vented cavity prevents the creation of the thermally isolated region and the heated region behind the heated baffles, due to the occupation of the isotherms behind the heated baffles. One can conclude that the location of the heated baffles enables the external flow to enhance heat transfer through the vented baffled heated cavity. The central location of the heated baffles plays an important role in the shape of the recirculation cell formed in the vented cavity as well as the one behind the upper heated cavity. The shape of the isotherms indicates that they are bifurcated in the heated region close to the two heated baffles and the left vertical heated wall. The main part of the isotherms are very tight in the vicinity of the left vertical heated wall and the upper heated baffle, Figure 4 (a-c). This situation indicates that the central position of the heated baffles contributes to the formation of the two equalized regions in the baffled vented cavity, where the cold region is still created in front of the heated baffles and the heated zone occupies the region close to the heated baffles and the heated left vertical wall. Then the natural convection dominates in the heated zone, by increasing Reynolds number.

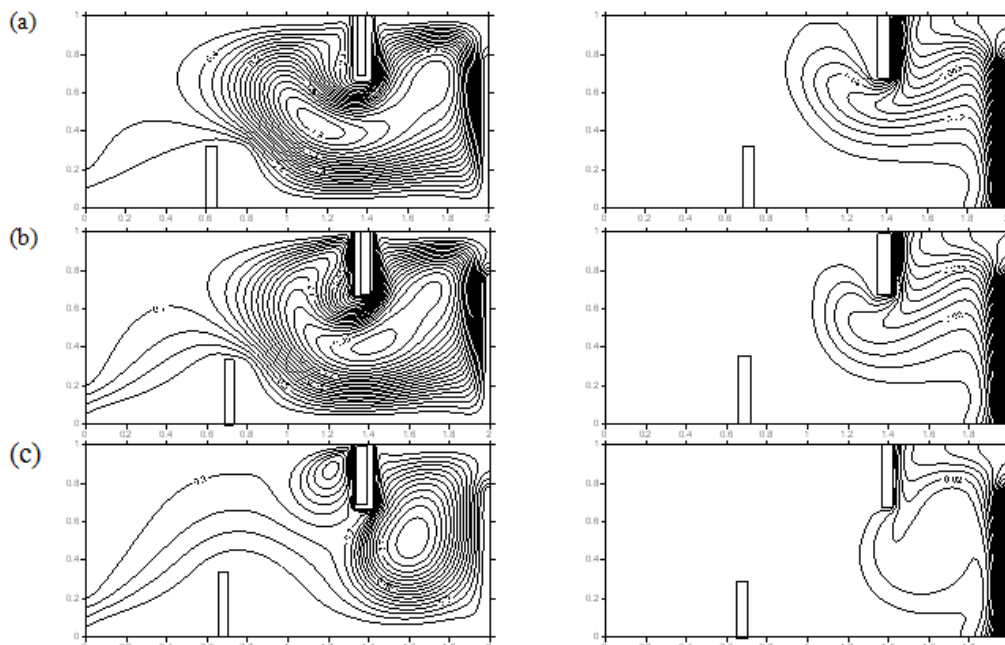


Figure 3. Streamline and isotherm distribution obtained for $Ra=10^6$, and different Reynolds numbers (a) $Re=10$, (b) $Re=20$; (c) $Re=50$

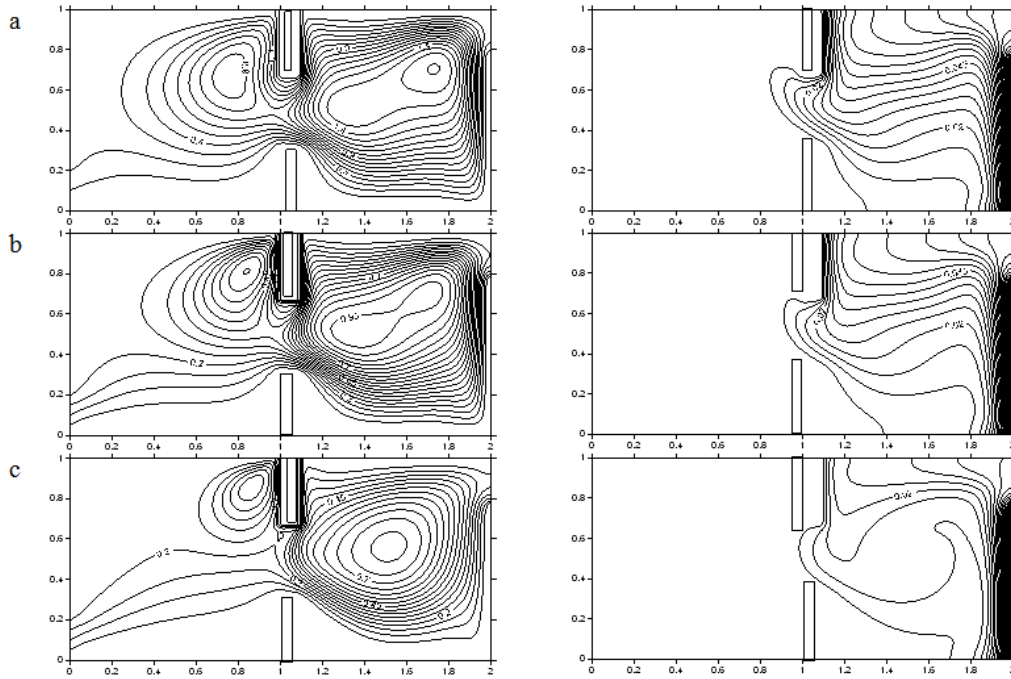


Figure 4. Streamline and isotherms distribution obtained for $Ra=10^6$, and different Reynolds numbers (a) $Re=10$, (b) $Re=20$; (c) $Re=50$

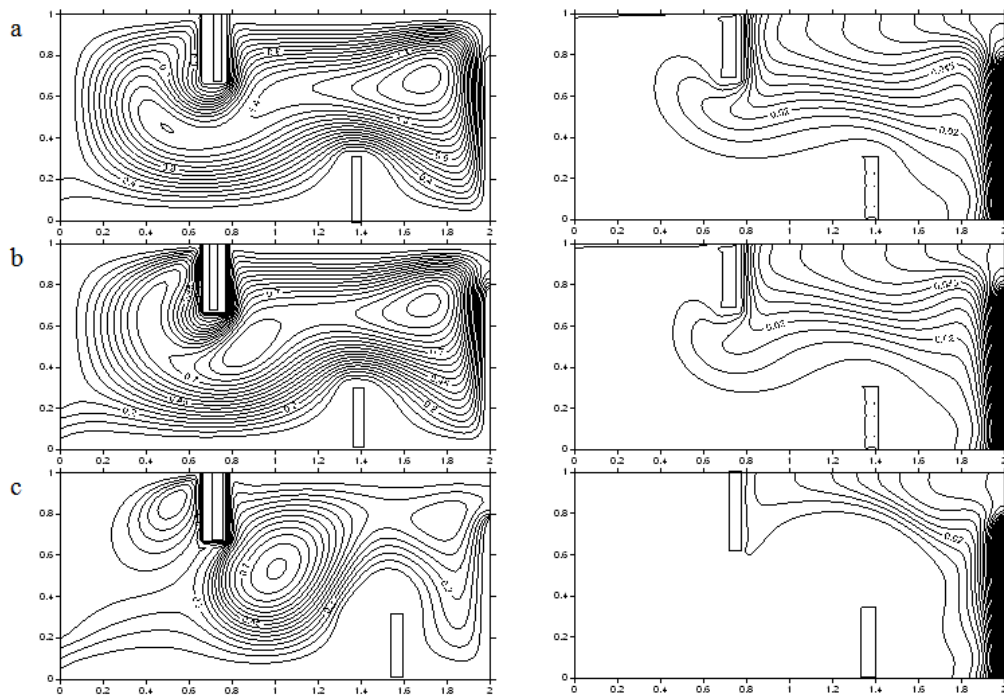


Figure 5. Streamline and isotherms distribution obtained for $Ra=10^6$, and different Reynolds numbers (a) $Re=10$; (b) $Re=20$; (c) $Re=50$

4.3. Streamline and Isotherm Distribution in the Configuration Case III: Baffles Right-left ($L/3$; $2L/3$)

Analysis of streamlines in Figure 5(a-c) obtained for a fixed Rayleigh number ($Ra=10^6$) for different values of Reynolds number, reveals the existence of open lines surmounted by the clockwise natural convection cell. For low values of Reynolds number, the big natural convective closed cell occupies the two zones in the baffled vented cavity. The size of the closed natural convective cell is decreasing until the formation of two closed cells in the respective zones when Reynolds

number is increasing, Figure 5(c). The corresponding isotherms are tightened at the level of the left vertical heated wall indicating good convective heat exchange between this wall and the open lines/(closed) cell on the left/(right) sides of the heated baffles. The cold zone is increasing while Reynolds number is increasing.

Figure 6 (a-c) shows that the intensity of the heat transfer along the left vertical heated wall increases with Reynolds number, for all the three configurations. The local Nusselt number is decreasing along the heated wall towards the minimum value before increasing to the maximum value near end ho wall of the vented cavity.

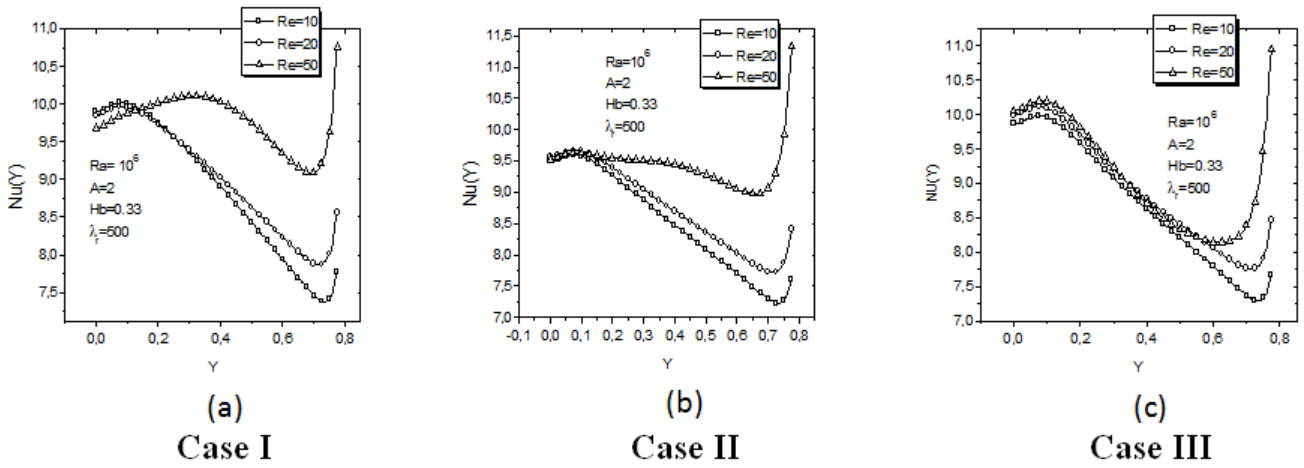


Figure 6. Variation of local Nusselt number along the left vertical heated wall

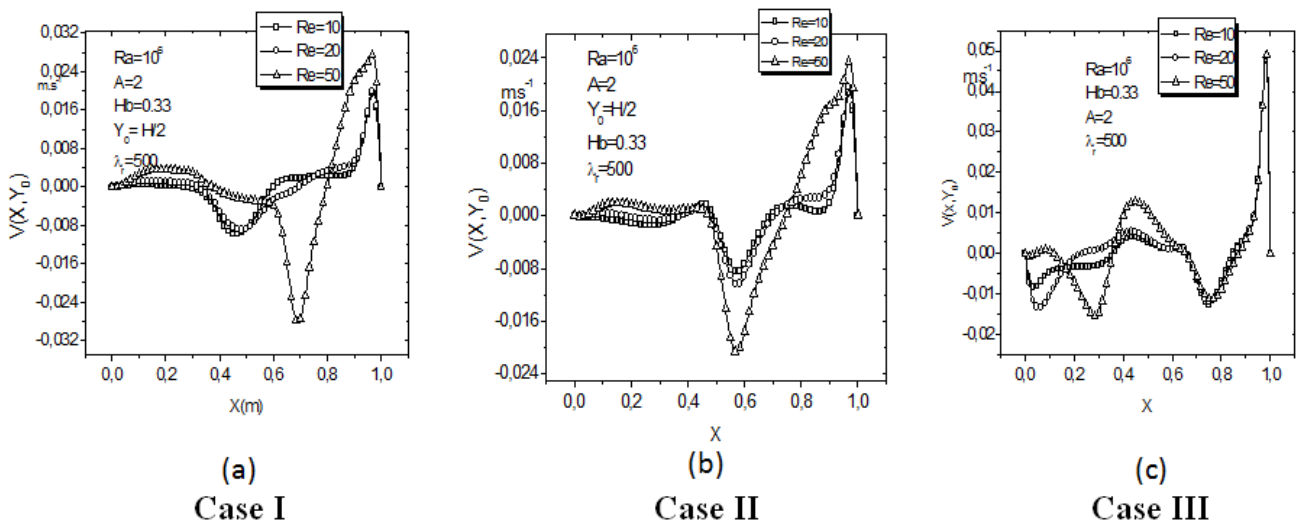


Figure 7. Variation of vertical velocity component for different Reynolds numbers

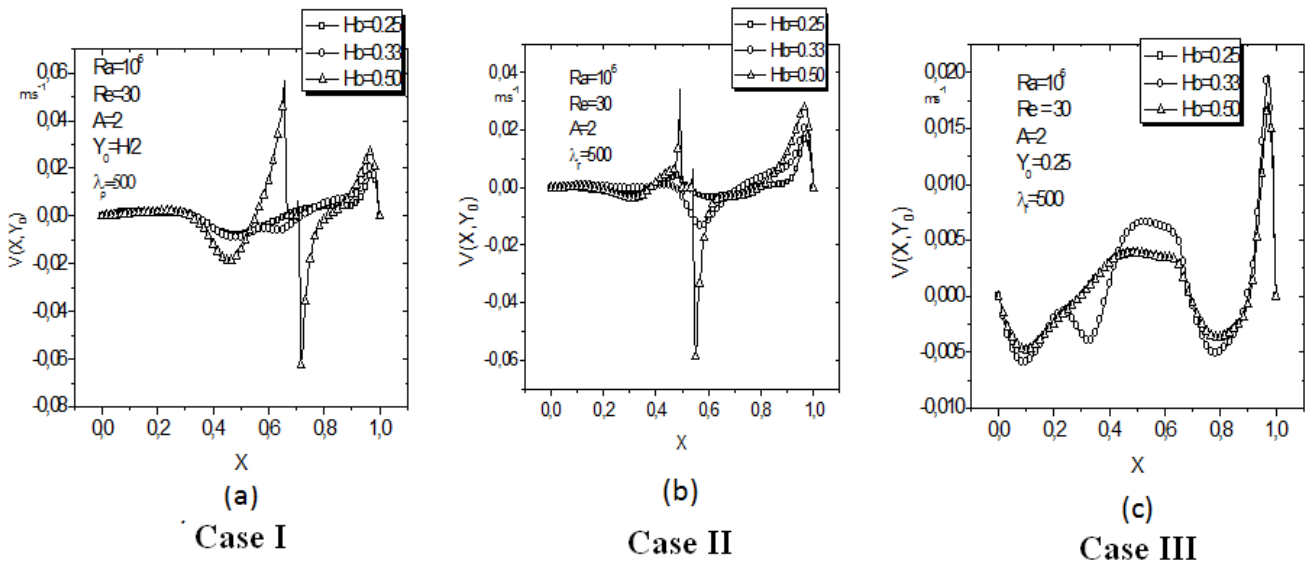


Figure 8. Variation of vertical velocity component for different values of the baffles height

Figure 7 shows the influence of Reynolds number on the variation of the vertical velocity component along the horizontal axis in the three configurations. In each configuration, the velocity decreases towards the minimum value and passes through the maximum value before

decreasing to attain zero near the left heated wall. The negatives values of the vertical velocity component means that there is a probably recirculation phenomenon in the baffled vented cavity. The recirculation of the cooling fluid is observed near the heated baffles and the left

vertical heating wall. Just close to the left vertical heated wall, the maximal value of the vertical velocity component is an increasing function of Reynolds number. The analysis of the vertical velocity component plots in the baffled vented configurations indicates that no slip conditions is verified along the walls.

4.4. Effect of Baffle Height

Figure 8 (a-c) shows the variation of the vertical velocity component for various heights of the baffles. Hence, one can observe that nearly the walls the velocity values tend to zero. This situation indicates that, no slip condition along the walls is observed. The negative values observed in the three cases for the effect of the baffles height indicate the proof of the existence of the recirculation zone in each configuration. The recirculation zone increases when the baffles height is increasing. In general the recirculation zone is located nearly the heated baffles. The maximum value of the vertical velocity component increases with baffles height.

As shown in Figure 9 (a-b), the intensity of heat transfer is increasing when the baffle height is increasing in the cases I, and II, while it is a decreasing function in the third configuration (case III), Figure 9(c).

The local Nusselt number had a peak just near the bottom of the heated wall and it tends towards the

minimum at the top of the heated wall and then increases drastically at the end of the heated wall, Figure 9 (a-c). This variation of the local Nusselt number indicates that baffle height plays an important role in enhancing the heat transfer in the electronic components box.

4.5. Effect of Rayleigh Number

As shown in Figure 10 (a-c), the vertical velocity component is an increasing function of Rayleigh number. One can observe the recirculation phenomenon of the coolant fluid particles in the three configurations.

The minimum values are attained just nearly the heated baffles while the maximum values are obtained through the exit opening. This tendency can be explained that the heat excess is evacuated via the exit located between the top horizontal adiabatic and the left vertical heated walls. The plot of the average Nusselt number along the left vertical heated wall in Figure 10 (a) allowed us to compare the heat enhancement from the location of the heated baffles in the vented cavity versus Rayleigh number. One observes that the heat enhancement is better in the configuration case I: **Baffles left- right (L/3; 2L/3)**. The same comparison is shown in Figure 11(b) where the highest heat transfer versus Reynolds number is obtained in the configuration case I(**Baffles left- right (L/3; 2L/3)**).

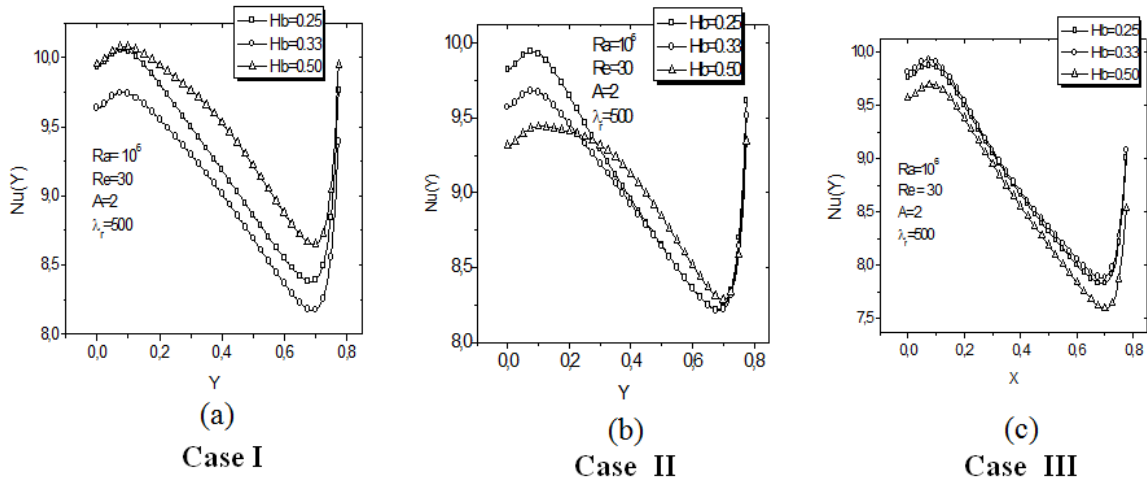


Figure 9. Variation of local Nusselt number for different values of baffle height

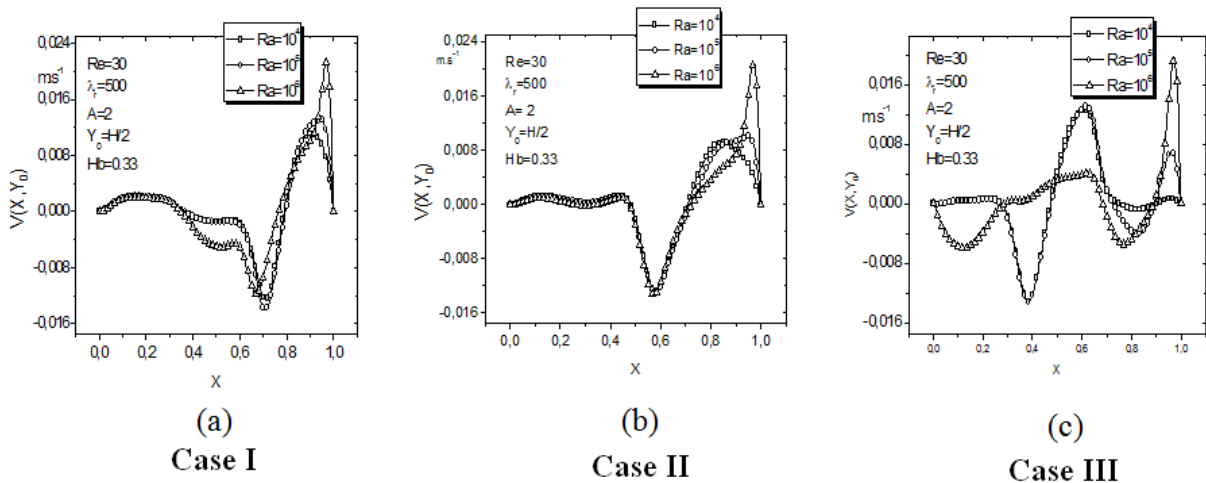


Figure 10. Variation of vertical velocity component for different Rayleigh numbers

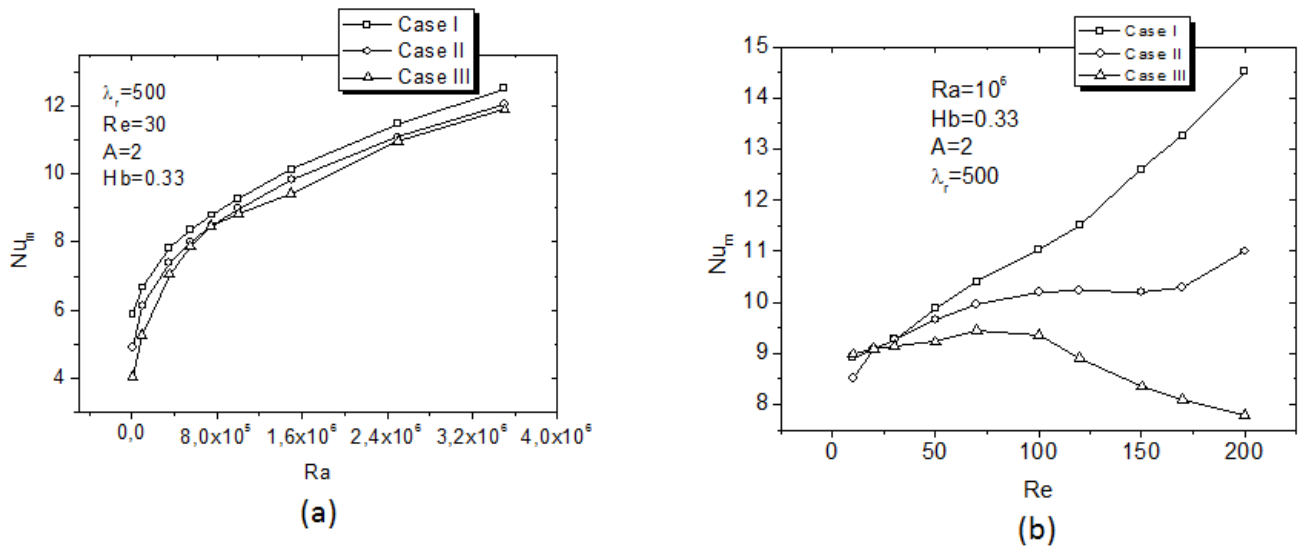


Figure 11. Variation of mean Nusselt number along the heated wall versus Rayleigh and Reynolds numbers

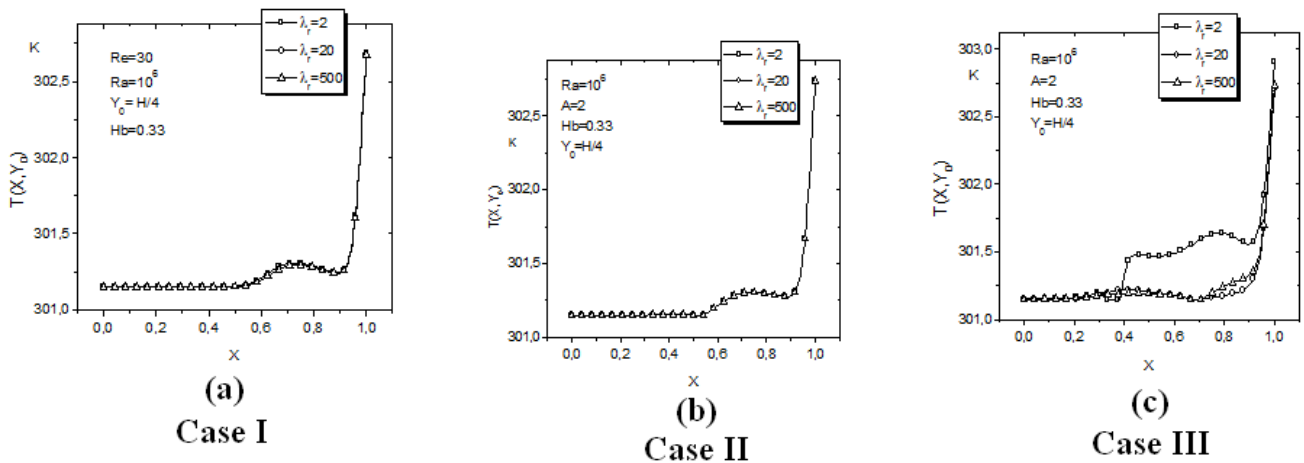


Figure 12. Variation of temperature versus relative conductivity coefficient

The location of the heated baffles **left- right** ($L/3; 2L/3$) enables several possibilities for electronic circuit aboard passive cooling. These results confirmed that location of the baffles in the vented cavity has an important effect on external flow and the heat transfer.

The effect of the relative conductivity coefficient is negligible on the variation of the dimensional temperature along the horizontal axis in the baffled vented cavity, Figure 12(a-c).

5. Conclusion

The authors analyzed the effect of the locations of the heated baffles on mixed convection in a vented cavity. Three configurations of the baffled vented cavity were considered.

The relative location of heated baffles **left-right** ($L/3; 2L/3$) gives several opportunities to obtain the optimum passive cooling effect for electronic circuit aboard.

In view of the results, we draw the following conclusions:

- Locations of the twice heated baffles along the horizontal walls give the possibility to create an isolated zone and the heated zone simultaneously

for industrial applications in the baffled vented cavity;

- Baffle locations play an important role on external flow in the baffled vented cavity;
- For external flow from the inlet opening, while increasing baffle height H_b , beyond 0.50 significantly affects heat transfer enhancement, the optimum height of baffle, should be around 0.50 to achieve maximum enhancement at any location of the heated baffles in the three configurations.
- The main interest for placing the baffles is to enhance heat transfer by diverting forced flow from the inlet opening to the exit, due to the cooling effect in the baffled vented cavity for industrial applications.

Nomenclature

- A Aspect ratio dimensionless of the global system $A = L/H$
- D Dimensionless aspect ratio of the total vertical wall $D = (h + e)/H$
- C_p Specific heat ($J \cdot kg^{-1} \cdot K^{-1}$)
- E Dimensionless aspect ratio of the inlet opening $E = e/H$

B Dimensionless aspect ratio of the remain vertical wall $B = h/H$

e Air inlet opening width (m)

a Thermal diffusivity ($\text{W.m}^{-2}.\text{K}^{-1}$)

a_r Relative thermal diffusivity $a_r = a_b/a$

g Gravitational acceleration (m.s^{-2})

H Total height of the cavity (m)

L Total length of the cavity (m)

n Coordinate in normal direction

Nu Nusselt number $Nu = \frac{\varnothing H}{\lambda(T_W - T_a)}$

Pr Prandtl number $Pr = \frac{\mu C_p}{\lambda}$

Re Reynolds number $Re = \frac{\rho u_0 (2e)}{\mu}$

Gr Grashof number $Gr = \frac{\rho^2 g \beta \varnothing (H)^4}{\lambda \mu^2}$

Ri Thermal Richardson number $Ri = \frac{Gr}{Re^2}$

t Time (s)

T Temperature (K)

T_a Ambient air temperature (K)

u, v Velocity component in x and y directions (m.s^{-1})

U, V Dimensionless velocity component in X and Y directions: $U = \frac{u}{u_0}$; $V = \frac{v}{u_0}$

u_0 Air inlet velocity (m.s^{-1})

W Dimensionless outlet velocity

x, y Coordinates defined in Figure 1 (m)

X, Y Dimensionless spatial coordinates $X = \frac{x}{H}$, $Y = \frac{y}{H}$

Greek symbols

θ Dimensionless temperature $\theta = \frac{\lambda(T - T_a)}{\varnothing H}$

θ_b Baffle dimensionless temperature $\theta_b = \frac{\lambda_b(T_b - T_a)}{\varnothing H}$

τ Dimensionless time $\tau = \frac{u_0 t}{H}$

β Thermal expansion coefficient (K^{-1})

ρ Density of the air (kg.m^{-3})

λ Air Thermal conductivity ($\text{W.m}^{-1}.\text{K}^{-1}$)

λ_b Baffle Thermal conductivity ($\text{W.m}^{-1}.\text{K}^{-1}$)

λ_r Relative thermal conductivity $\lambda_r = \lambda_b/\lambda$

Ω Vorticity (s^{-1})

ω Dimensionless vorticity $\omega = \frac{\Omega H}{u_0}$

μ Dynamic viscosity of the air ($\text{kg.m}^{-1}.\text{s}^{-1}$)

ψ Stream function ($\text{m}^2.\text{s}^{-1}$)

Ψ Dimensionless stream function $\Psi = \frac{\psi}{u_0 H}$

ϕ Solar radiation (W.m^{-2})

Subscripts

w Wall

f Fluid (air)

b baffle.

References

- [1] Du S-Q, Bilgen E and Vasseur P 1998 Mixed convection heat transfer in open ended channels with protruding heaters. *Heat Mass Transfer* 34: 263-270.
- [2] How S-P and Hsu T-H 1998 Transient mixed convection in a partially divided enclosure. *Computers Math.Applic.* 36: 95-115.
- [3] Hsu T H and How S P 1999 Mixed convection in an enclosure with a heat-conducting body. *Acta Mechanica* 133: 87-104.
- [4] El-din M M S 2002 Effect of viscous dissipation on fully developed laminar mixed convection in a vertical double-passage channel. *Int. J. Thermal Sci.* 41: 253-259.
- [5] Manca O, Nardini S, Khanafar K and Vafai K 2003 Effect of heated wall position on mixed convection in a channel with an open cavity. *Numer. Heat Transfer A* 43: 259-282.
- [6] Singh S. and Sharif M. A. R. 2003, Mixed convective cooling of a rectangular cavity with inlet and exit openings on differentially heated side walls. *Numer. Heat Transfer A* 44: 233-253.
- [7] Raji A, Hasnaoui M and Bahlaoui A 2008 Numerical study of natural convection dominated heat transfer in a ventilated cavity: Case of forced flow playing simultaneous assisting and opposing roles. *Int. J. Heat Fluid Flow* 29: 1174-1181.
- [8] Bahlaoui A, Raji A, Hasnaoui M, Naïmi M, Makayssi T and Lamsaadi M 2009 Mixed convection cooling combined with surface radiation in a partitioned rectangular cavity. *Energy Conv. Management* 50: 626-635.
- [9] Chang T-S and Shiau Y-H 2005 Flow pulsation and baffles effects on the opposing mixed convection in a vertical channel. *Inter. J. Heat Mass Transfer* 48: 4190-4204.
- [10] Chung C K, Wu C-Y and Shih T R 2008 Effect of baffle height and Reynolds number on fluid mixing. *Microsyst. Technol.* 14: 1317-1323.
- [11] Radhakrishnan T V, Joseph G, Balaji C and Venkateshan S P 2009 Effect of baffle on convective heat transfer from a heat generating element in a ventilated cavity. *Heat Mass Transfer* 45: 1069-1082.
- [12] Asif M R, Hossain M S and Hossain K A 2011 Heat Transfer in a rectangular enclosure with baffles. *ARPN J. Eng. Appl. Sci.* 6: 29-41.
- [13] Sripattanapipat S and Promvong P 2009 Numerical analysis of laminar heat transfer in a channel with diamond-shaped baffles. *Int. Commun. Heat Mass Transfer* 36: 32-38.
- [14] Sriromreun P, Thianpong C and Promvong P 2012 Experimental and numerical study on heat transfer enhancement in a channel with Z-shaped baffles. *Int. Commun. Heat Mass Transfer* 39: 945-952.
- [15] Manca O, Nardini S and Vafai K 2008 Experimental investigation of opposing mixed convection in a channel with an open cavity below. *Exper. Heat Transfer* 21: 99-114.
- [16] Woods L.C. 1954. A note of numerical solution of fourth differential equations, *Aero. Q.* 5, 176-184.
- [17] Sumon Saha Md. Tofiqul Islam, Mohammad Ali, Md. Arif Hasan Mamun and M. Quamrul Islam, 2006. Effect of inlet and outlet locations on transverse mixed convection inside a vented enclosure. *Journal of Mechanical Engineering, vol. ME36, Dec. 2006.* PP 27- 37.

